

Claremont Colleges Scholarship @ Claremont

CMC Senior Theses

CMC Student Scholarship

2011

Twisted Virtual Biracks

Jessica Ceniceros
Claremont McKenna College

Recommended Citation

Ceniceros, Jessica, "Twisted Virtual Biracks" (2011). *CMC Senior Theses*. Paper 176.
http://scholarship.claremont.edu/cmc_theses/176

This Open Access Senior Thesis is brought to you by Scholarship@Claremont. It has been accepted for inclusion in this collection by an authorized administrator. For more information, please contact scholarship@cuc.claremont.edu.

CLAREMONT McKENNA COLLEGE

TWISTED VIRTUAL BIRACKS

SUBMITTED TO

PROFESSOR SAM NELSON

AND

DEAN GREGORY HESS

BY

JESSICA CENICEROS

FOR

SENIOR THESIS

FALL '10/SPRING '11

APRIL 25, 2011

Abstract

This thesis will take a look at a branch of topology called knot theory. We will first look at what started the study of this field, classical knot theory. Knot invariants such as the Bracket polynomial and the Jones polynomial will be introduced and studied. We will then explore racks and biracks along with the axioms obtained from the Reidemeister moves. We will then move on to generalize classical knot theory to what is now known as virtual knot theory which was first introduced by Louis Kauffman. Finally, we take a look at a newer aspect of knot theory, twisted virtual knot theory and we defined new link invariants for twisted virtual biracks.

Contents

- Introduction 2
- 1 Classical Knot Theory 3**
 - 1.1 Bracket Polynomial 3
 - 1.2 Racks 6
 - 1.3 Biracks 7
- 2 Virtual Knot Theory 10**
 - 2.1 Defining Virtual Knots 10
 - 2.2 Gauss Codes 12
 - 2.3 Bracket Polynomial 12
 - 2.4 Biracks 13
 - 2.5 (t, s, r) -biracks 14
- 3 Twisted Virtual Links 16**
 - 3.1 Twisted Jones Polynomial 19
 - 3.2 Twisted Virtual Biracks 19
 - 3.3 Counting Invariants 22
 - 3.4 Enhanced Counting Invariants 24

Introduction

In [9, 7] *virtual knots and links* and similarly *abstract knots links* were introduced, respectively. Virtual knots were initially thought of as combinatorial objects, and Reidemeister equivalence classes of Gauss codes, where abstract knots were geometric in nature, knot diagrams were drawn on minimalistic supporting surfaces. In [5] a geometric interpretation of virtual and abstract links as isotopy classes of simple closed curves in I -bundles over compact oriented surfaces modulo stabilization moves was developed.

In recent work such as [2, 8], virtual and abstract links are extended to allow compact non-orientable supporting surfaces; the resulting links are called *twisted virtual links*. Invariants of twisted virtual links such as the twisted Jones polynomial and the twisted knot group have been introduced and studied.

Quandle- and biquandle-based invariants of twisted virtual links were first considered in [14]. In [12] a counting invariant of unframed oriented classical and virtual knots and links was defined using labelings by finite racks and extended to finite biracks in [13]. The latter part of this thesis will extend the birack counting invariant to the case of twisted virtual links.

Chapter 1

Classical Knot Theory

A *knot* is defined as a simple closed curve in \mathbb{R}^3 . A *knot diagram* is the projection of a knot onto a plane with over and under crossings. A *link* is made up of one or more components so for example a knot is a link with one component. In the late 1920's Kurt Reidemeister showed that knots can be equivalent up to isotopy with a combination of moves that are now known as Reidemeister Moves.

The motivation behind knot theory is to be able to distinguish between different knots. To make this distinction we have what are called knot invariants. A *knot invariant* is a quantity that is defined for each knot and is the same if the knots are equivalent up to ambient isotopy. The knot invariant can range from a number up to a polynomial. The first knot polynomial discovered was in 1923 by James Waddell Alexander II appropriately known as the Alexander polynomial. Then in 1969, John Conway showed a variation of this polynomial using a skein relation but its significance was not realized until the discovery of the Jones polynomial in 1984.

1.1 Bracket Polynomial

Before introducing the Jones polynomial formally, we will introduce the Bracket polynomial. An *oriented* link has a direction on each of its components indicated by arrows on its arcs. Oriented crossings are given *signs* of ± 1 , $+1$ if the under crossing is going from right to left and -1 if the under crossing is going from left to right. The *writhe*, denoted as $w(L)$, is defined as the sum of all the crossing of the oriented link as one traverses through the link.

Now we begin by introducing the Bracket polynomial.

Definition 1 Let L be an unoriented link diagram and let L be the element of the ring $\mathbb{Z}[A, A^{-1}, -A^2, -A^{-2}]$ defined by:

1. $\langle O \rangle = 1$
2. $\langle O \cup L \rangle = (-A^2 - A^{-2}) \langle L \rangle$ (where $L \neq \emptyset$)
3. $\langle \begin{array}{c} \nearrow \searrow \\ \nwarrow \nearrow \end{array} \rangle = A \langle \begin{array}{c} \frown \\ \smile \end{array} \rangle + A^{-1} \langle \begin{array}{c} \rangle \\ \langle \end{array} \rangle$, or
 $\langle \begin{array}{c} \nwarrow \nearrow \\ \nearrow \searrow \end{array} \rangle = A \langle \begin{array}{c} \rangle \\ \langle \end{array} \rangle + A^{-1} \langle \begin{array}{c} \frown \\ \smile \end{array} \rangle$.

In [1], Kauffman showed that the Bracket polynomial is invariant under Reidemeister moves II and III but an interesting thing happens under Reidemeister move I.

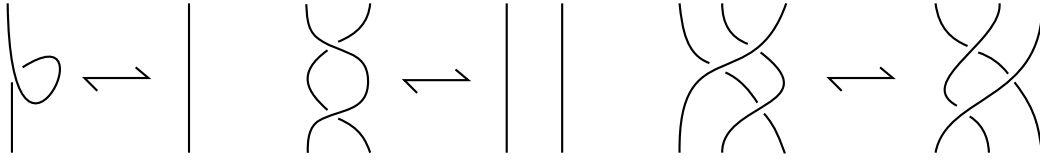
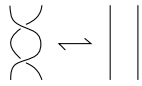


Figure 1.1: Reidemeister Moves I, II, and III

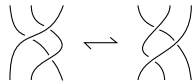
Let's begin by illustrating invariance of the Bracket polynomial under R-moves II and III:

- R-move II:



$$\begin{aligned}
 &= A \langle \text{crossing} \rangle + A^{-1} \langle \text{crossing} \rangle \\
 &= A(A \langle \text{crossing} \rangle + A^{-1} \langle \text{crossing} \rangle) + A^{-1}(A \langle \text{crossing} \rangle + A^{-1} \langle \text{crossing} \rangle) \\
 &= A^2 \langle \text{crossing} \rangle + AA^{-1} \langle \text{crossing} \rangle + AA^{-1} \langle \text{crossing} \rangle + A^{-2} \langle \text{crossing} \rangle \\
 &= A^2 \langle \text{crossing} \rangle + AA^{-1}(-A^2 - A^{-2}) \langle \text{crossing} \rangle + AA^{-1} \langle \text{crossing} \rangle + A^{-2} \langle \text{crossing} \rangle \\
 &= AA^{-1} \langle \text{crossing} \rangle = \langle \text{crossing} \rangle
 \end{aligned}$$

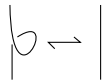
- R-move III:



$$\begin{aligned}
 &= A \langle \text{crossing} \rangle + A^{-1} \langle \text{crossing} \rangle \\
 &= A \langle \text{crossing} \rangle + A^{-1} \langle \text{crossing} \rangle \\
 &= \langle \text{crossing} \rangle
 \end{aligned}$$

Now we will see what happens when we compute the Bracket polynomial for Reidemeister move I:

- R-move I



$$\begin{aligned}
 &= A \langle \text{loop} \rangle + A^{-1} \langle \text{loop} \rangle \\
 &= A \langle \text{loop} \rangle + A^{-1}(-A^2 - A^{-2}) \langle \text{loop} \rangle \\
 &= (A - A - A^{-3}) \langle \text{loop} \rangle \\
 &= -A^{-3} \langle \text{loop} \rangle
 \end{aligned}$$



Figure 1.2: Negative and positive crossing, respectively

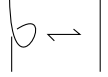
As we can see we get the extra term, $-A^{-3}$ therefore to fix this we will now define the X polynomial.

Definition 2 The *X polynomial* is a polynomial of oriented links and is defined to be

$$X(L) = (-A^3)^{-w(L)} \langle L \rangle$$

Since neither $w(L)$ nor $\langle L \rangle$ are affected by moves II and III, $X(L)$ is unaffected by moves II and III and we will subsequently see that $X(L)$ is also unaffected by move I.

Let's see what happens to $X(L)$ when we look at Reidemeister move I:



$$\text{Let } W\langle \text{loop} \rangle = W - 1 \quad \text{and} \quad W\langle \rangle = W$$

We know from the previous result that $\langle \text{loop} \rangle = -A^{-3} \langle \rangle$. Then,

$$\begin{aligned} X\langle \text{loop} \rangle &= (-A^3)^{-W\langle \text{loop} \rangle} \langle \text{loop} \rangle \\ &= (-A^3)^{-W\langle \rangle+1} (-A^{-3}) \langle \rangle \\ &= (-A^3)^{-W\langle \rangle} (-A^3) (-A^{-3}) \langle \rangle \\ &= (-A^3)^{-W\langle \rangle} \langle \rangle \\ &= X\langle \rangle \end{aligned}$$

As we can see, $X(L)$ is in fact not affected by R-move I.

We will now focus on showing how to compute the Jones polynomial for the trefoil knot; the smallest nontrivial knot.

We begin by computing the bracket polynomials for both the Hopf link and the trefoil knot then using the Bracket polynomial of the Hopf link to help us compute the Jones polynomial for the trefoil knot.

Starting from one crossing let us begin the computation:

$$\begin{aligned} \text{Example 1 } \langle \text{crossing} \rangle &= A \langle \text{loop} \rangle + A^{-1} \langle \text{infinity} \rangle \\ &= A(A \langle \text{circle} \rangle + A^{-1} \langle \text{circle} \rangle) + A^{-1} \langle \text{infinity} \rangle \\ &= A(A(-A^2 - A^{-2}) + A^{-1}) + A^{-1} \langle \text{infinity} \rangle \\ &= A(-A^3 - A^{-1} + A^{-1}) + A^{-1} \langle \text{infinity} \rangle \\ &= -A^4 + A^{-1} \langle \text{infinity} \rangle \\ &= -A^4 + A^{-1}(A \langle \text{circle} \rangle + A^{-1} \langle \text{circle} \rangle) \\ &= -A^4 + A^{-1}(A + A^{-1}(-A^2 - A^{-2})) \\ &= -A^4 - A^{-4} \end{aligned}$$

$$\begin{aligned} \text{Example 2 } \langle \text{trefoil} \rangle &= A \langle \text{circle} \rangle + A^{-1} \langle \text{trefoil} \rangle \\ &= A(-A^4 - A^{-4}) + A^{-7} \\ &= (A^{-7} - A^{-3} - A^5) \end{aligned}$$

Definition 3 Let the Bracket polynomial be denoted as $\langle L \rangle (A)$ then the *Jones polynomial* is defined as

$$V(t) = (-A^3)^{-w(L)} \langle L \rangle (A) \text{ where } A = t^{-1/4}$$

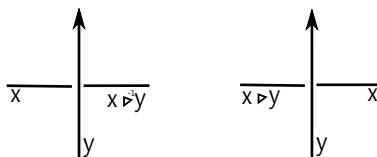
The trefoil's writhe is +3 (if looking at its mirror image the writhe would be -3).

We then have that the Jones polynomial for the trefoil knot is

$$\begin{aligned} V(t) &= (-A^3)^{-3}(A^{-7} - A^{-3} - A^5) \\ &= -A^{-16} + A^{-12} + A^{-4} \text{ with } A = t^{-1/4} \\ V(t) &= t + t^3 - t^4 \end{aligned}$$

1.2 Racks

This section begins with the introduction of racks and quandles which correspond to Reidemeister moves II and III. We can think of rack elements as arcs in an oriented link diagram where the binary operation, \triangleright , means crossing under from right to left when looking at the positive crossing and the operation \triangleright^{-1} can then be thought of as crossing under from left to right.



Definition 4 A *rack* is a set X with a binary operation $\triangleright: X \times X \rightarrow X$ satisfying

1. for all $x, y \in X$ there is a unique $z \in X$ satisfying $x = z \triangleright y$, and
2. for all $x, y, z \in X$ we have $(x \triangleright y) \triangleright z = (x \triangleright z) \triangleright (y \triangleright z)$.

A rack in which $x \triangleright x = x$ is a *quandle*, i.e., its rack rank is 1.

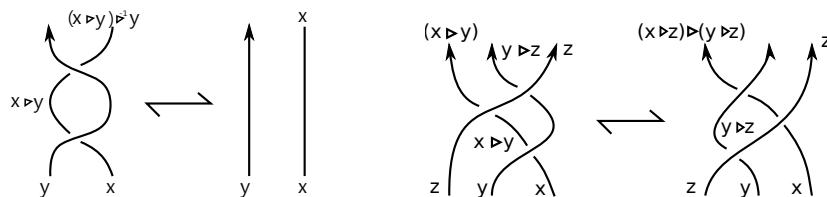


Figure 1.3: Rack axioms I and II

Example 3 The following example is from [12] in which the *constant action rack* or *permutation rack* is introduced. Let the constant action rack be a rack structure on a finite set $R = \{x_1, \dots, x_n\}$ associated to a permutation $\sigma \in S_n$. Set

$$x_i \triangleright x_j = x_{\sigma(i)}$$

for all $i = 1, \dots, n$. This definition gives us a rack structure since $x_i \triangleright^{-1} x_j = x_{\sigma^{-1}(i)}$ and we have

$$(x_i \triangleright x_j) \triangleright x_k = x_{\sigma^2(i)} = (x_i \triangleright x_k) \triangleright (x_j \triangleright x_k).$$

Further, the constant action rack on $R = \{x_1, x_2, x_3\}$ defined by $\sigma = (123)$ has matrix

$$M(123) = \begin{bmatrix} 2 & 2 & 2 \\ 3 & 3 & 3 \\ 1 & 1 & 1 \end{bmatrix}$$

Where rack axiom 1 requires the columns of a rack matrix to be permutations.

1.3 Biracks

Reidemeister moves were translated into algebraic axioms by assigning algebraic generators to arcs in a knot diagram and viewing crossings as operations. Applying this idea to oriented link diagrams gives us the quandle structure. Generalizing again to blackboard-framed diagrams gives us the rack structure. Further generalization replaces *arcs*, portions of the knot diagram from one undercrossing point to another, with *semiarcs*, portions of the knot diagram from one over or under crossing point to the next. Semiarc-generated algebraic structures from unframed oriented link diagrams are known as *biquandles*.

Biracks are algebraic structures generated by semiarcs in a link diagram with axioms corresponding to blackboard framed isotopy. Before dening biracks formally, a few more definitions are needed. From [13],

Definition 5 Let X be a set. A map $B : X \times X \rightarrow X \times X$ is *strongly invertible* if B satisfies the following three conditions:

- B is invertible, i.e., there exists a map $B^{-1} : X \times X \rightarrow X \times X$ satisfying $B \circ B^{-1} = Id_{X \times X} = B^{-1} \circ B$
- B is *sideways invertible*, there exists a unique invertible map $S : X \times X \rightarrow X \times X$ satisfying

$$S(B_1(x, y), x) = (B_2(x, y), y),$$

for all $x, y \in X$, and

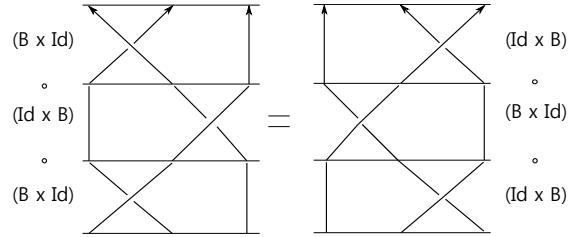
- The maps S and S^{-1} are *diagonally bijective*, i.e., the compositions $S_1^\pm \circ \Delta$, $S_2^\pm \circ \Delta$ of the components of S and S^{-1} with the map $\Delta : X \rightarrow X \times X$ defined by $\Delta(x) = (x, x)$ are bijections.

We can now go on to define a birack formally.

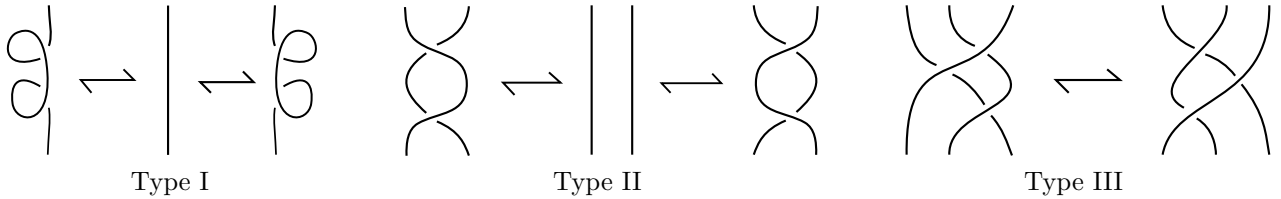
Definition 6 A *birack* (X, B) is a set X with an invertible map $B : X \times X \rightarrow X \times X$ which satisfies the *set-theoretic Yang-Baxter* equation

$$(B \times Id) \circ (Id \times B) \circ (B \times Id) = (Id \times B) \circ (B \times Id) \circ (Id \times B)$$

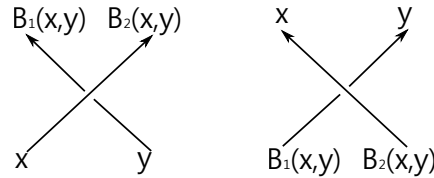
The idea that B is a solution to the set-theoretic Yang-Baxter equation arises from the condition that labeling under Reidemeister move III is preserved with Cartesian product \times showing horizontal stacking, and composition \circ indicating vertical stacking.



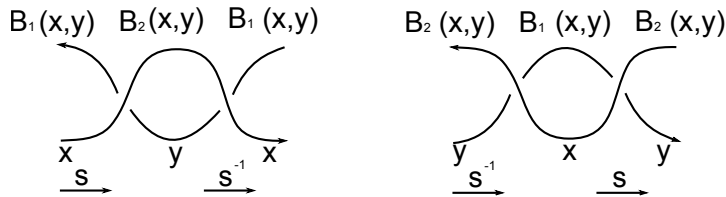
A *blackboard-framed link* is an equivalence class of link diagrams under the equivalence relation generated by the blackboard-framed Reidemeister moves:



The birack axioms stem from the labeling of the semiarcs in an oriented blackboard-framed link diagram with elements of X satisfying the following:



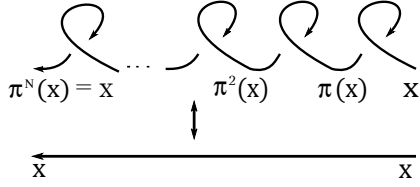
such that they correspond to a unique labeling of any of the blackboard-framed Reidemeister moves.



In order to acquire well-defined counting invariants we must satisfy the *strong birack* condition, that is, the component maps B_1 and B_2 of B are left and right invertible, respectively.

Definition 7 From [13], let (X, B) be a birack. Then the *kink map* of (X, B) is the bijection $\pi : X \rightarrow X$ given by $\pi = S_1^{-1} \circ \Delta \circ (S_2^{-1} \circ \Delta)^{-1}$, where $\pi(x)$ represents going through a positive kink.

Definition 8 Let (X, B) be a birack and let $\pi : X \rightarrow X$ be the kink map. The *birack rank* of (X, B) , denoted N , is the smallest positive integer N such that $\pi^N(x) = x$ for all $x \in X$.



Example 4 An example of a birack is a *constant action birack*. Let X be any set and let $\rho, \tau : X \rightarrow X$ be bijections. Then provided ρ and τ commute, $B(x, y) = (\tau(y), \rho(x))$ defines a birack. The Yang-Baxter components then become

$$\rho^2(x) = \rho^2(x), \quad \tau\rho(y) = \rho\tau(y), \quad \text{and} \quad \tau^2(z) = \tau^2(z).$$

Additionally, we have that $B^{-1}(x, y) = (\rho^{-1}(y), \tau^{-1}(x))$, $S(u, v) = (\rho(u), \tau^{-1}(u))$ with $S^{-1}(u, v) = (\tau(v), \rho^{-1}(u))$, $f(x) = \tau^{-1}(x)$ and $g(x) = \rho(x)$. The kink map is $\pi(x) = \rho\tau^{-1}(x)$, so N is the order of the permutation $\rho\tau^{-1}$ in the symmetric group $S_{|x|}$.

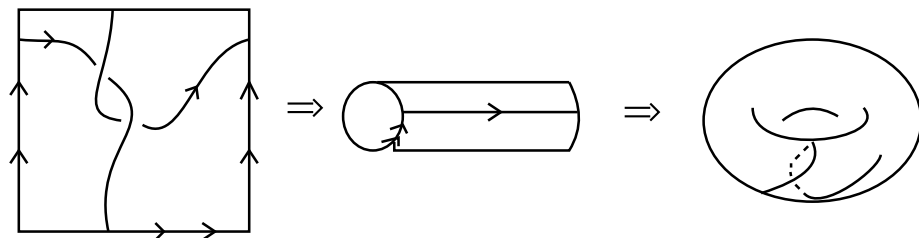
Chapter 2

Virtual Knot Theory

Virtual Knot theory was first introduced by Louis Kauffman, see [9]. Virtual knot theory can be regarded as a projection of classical knot theory but in thickened surfaces. The rules for working with virtual knots can be brought on by the idea of a knot diagram to its Gauss code.

2.1 Defining Virtual Knots

In a *virtual diagram* we allow a new crossing as a 4-valent vertex with a small circle around it to draw non-planar graphs. Just as in the case of classical knots, virtual knots are obtained as equivalence classes under the equivalence relation generated by the Reidemeister moves. In this case we allow an extra Reidemeister move which involves a classical crossing and two virtual crossings. However, two potential moves are not allowed, the *forbidden moves*, F_1 and F_2 . Unlike the other virtual moves, the two forbidden moves can be used to unknot any knot, virtual or classical.



To better understand the concept behind a virtual crossing, imagining a knot embedded on a torus facilitates the understanding. On the surface of the torus the knot will be actually crossing, perhaps on the top, as well as on the bottom, but when the knot is projected on to a plane, the crossings from the top and bottom portions may appear to be crossing when in fact they are not. This type of crossing is the virtual crossing.

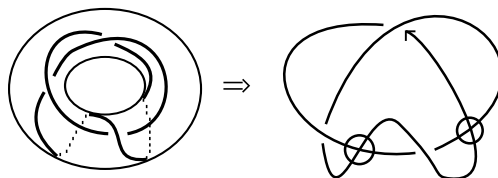


Figure 2.1: A knot on a torus and its diagram

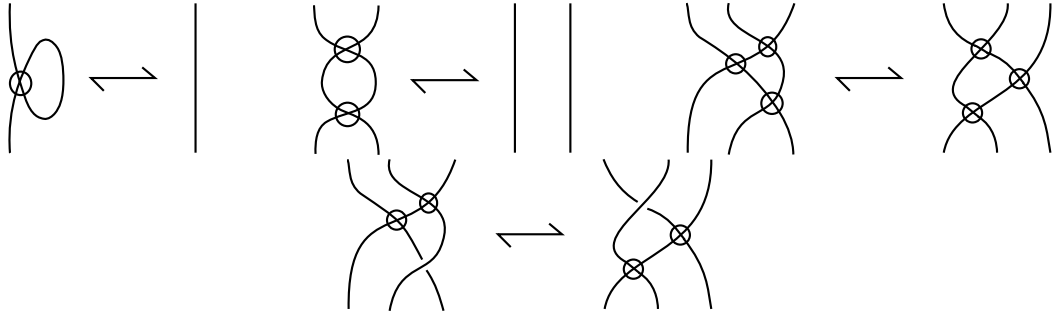


Figure 2.2: Virtual Reidemeister Moves I, II, III and V

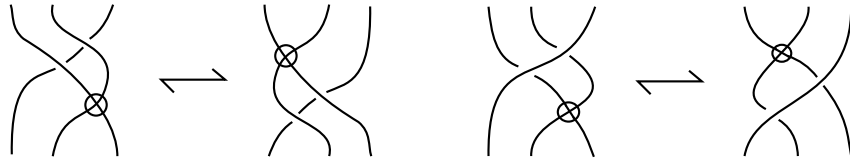


Figure 2.3: Forbidden moves F_1 and F_2

2.2 Gauss Codes

We now move on to another motivation and this comes from the use of *Gauss codes* to represent knots. The idea behind the Gauss code is to label the knot diagram at each crossing as you traverse through the knot. When writing out the code, we begin anywhere on the knot and go through all the crossings denoting whether the labeling is an over or undercrossing with O, or U, respectively. In the case of a virtual crossing, we do not label the crossing and we just go through it. When we have a link of two or more components then we go through all the components denoting the end of one component with ‘/’.

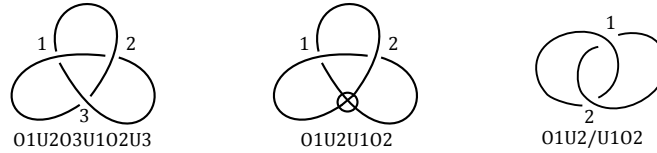


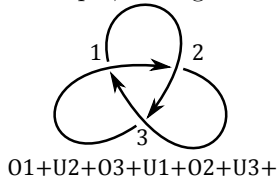
Figure 2.4: Gauss codes for planar and non-planar diagrams

Definition 9 A Gauss code g of a single component is *evenly intersticed* if there is an even number of labels in between the two appearances of any label.

Lemma 1 From [9], if g is a single component planar Gauss code, then g is evenly intersticed.

Adding an orientation to the knot, one can give a crossing a sign relative to the starting point of the code. We assign a sign of +1 or -1 according to the same rule of positive or negative crossings in the classical case.

For example, the signed Gauss code for the trefoil is



2.3 Bracket Polynomial

Just as in the classical case, the Bracket polynomial extends nicely to the virtual case if we trivialize the virtual crossing and as a result we use the same rules for the Bracket polynomial as in the classical case. We can see that the Bracket polynomial is invariant under the virtual Reidemeister moves because the virtual crossings do not disturb the loop count and so leave the bracket invariant. Virtual Reidemeister v is similarly invariant as classical Reidemeister move III:

$$\begin{aligned}
 & \bullet \quad \begin{array}{c} \text{Diagram 1} \\ \longleftrightarrow \\ \text{Diagram 2} \end{array} \\
 & = A \langle \text{Diagram 3} \rangle + A^{-1} \langle \text{Diagram 4} \rangle \\
 & = A \langle \text{Diagram 5} \rangle + A^{-1} \langle \text{Diagram 6} \rangle = \text{Diagram 7}
 \end{aligned}$$

Example 5 The Bracket polynomial of the virtual trefoil knot is:

$$\begin{aligned}
 \langle \text{trefoil} \rangle &= A \langle \text{two crossings} \rangle + \langle \text{one crossing} \rangle \\
 &= A(A \langle \text{one crossing} \rangle + A^{-1} \langle \text{one crossing} \rangle) + A^{-1}(A \langle \text{one crossing} \rangle + A^{-1} \langle \text{two crossings} \rangle) \\
 &= A(A + A^{-1}) + A^{-1}(A + A^{-1}(-A^2 - A^{-2})) \\
 &= A^2 + 1 + 1 - 1 - A^{-4} \\
 &= A^2 + 1 - A^{-4}
 \end{aligned}$$

From [9], we can define the f -polynomial by

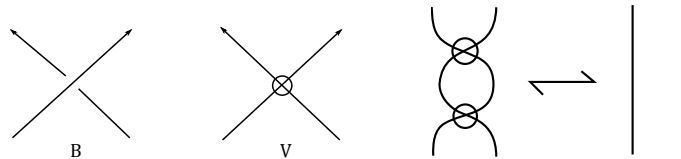
$$f_K(A) = (-A^3)^{-w(K)} \langle K \rangle (A)$$

where we define $w(K)$, the writhe, for oriented virtual links just the same as in the classical case. The Jones polynomial is obtained in a similar fashion as for classical knots.

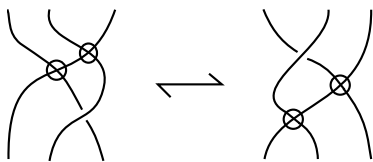
2.4 Biracks

We now go on to define virtual biracks.

Definition 10 A set X with two birack structures is a *virtual birack* if:



- B and V have to be compatible via



- And the Yang-Baxter equation:

$$(B \times Id_x)(Id_x \times V)(V \times Id_x) = (Id_x \times V)(V \times Id_x)(Id_x \times B)$$

needs to be satisfied.

Figure 2.5 demonstrates the virtual biracks where the virtual crossing is trivial.

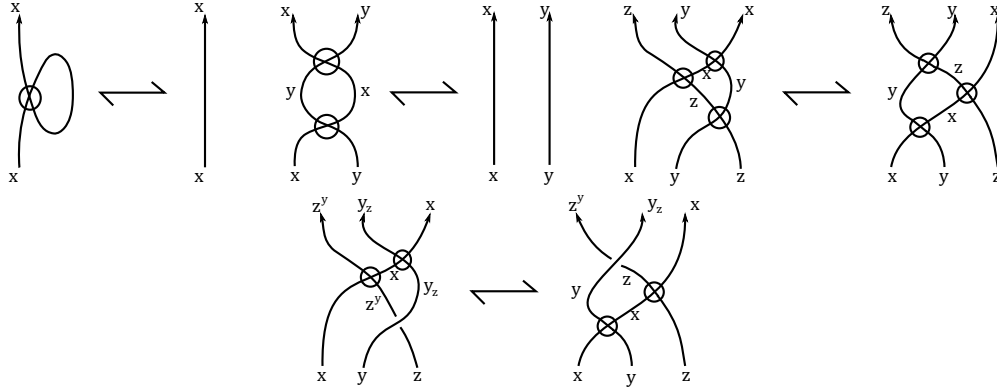
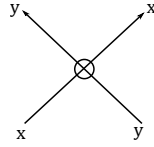


Figure 2.5: Virtual birack axioms

Definition 11 Any oriented blackboard-framed link diagram $L = L_1 \cup \dots \cup L_c$ has a *fundamental birack* denoted $BR(L)$. The fundamental birack $BR(L)$ of the link L is the set of equivalence classes of free blackboard birack elements under the additional equivalence relation generated by the crossing relations in L . Generally the birack of G is expressed by $BR(L) = \langle G | R \rangle$ where G is the set of arc labels and R is the set of crossing relations.

We let the virtual crossing be trivial to get



then we have $V(x, y) = (y, x)$

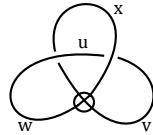


Figure 2.6: $BR(L) = \langle w, v, u, x | B(w, v) = (u, x), B(u, x) = (w, v) \rangle$

2.5 (t, s, r) -biracks

From [13], we define a class of biracks called (t, s, r) -biracks. Let $\tilde{\Lambda} = \mathbb{Z}[t^{\pm 1}, s, r^{\pm 1}] / I$ where I is the ideal generated by $s^2 - (1 - tr)s$ and let X be any $\tilde{\Lambda}$ module.

Proposition 2 Let X be a $\tilde{\Lambda}$ -module and define $B(x, y) = (ty + sx, rx)$. Then (X, B) is a birack with kink map $\pi(x) = (tr + s)x$.

Proof. First we need to check that B is strongly invertible. We see that $B^{-1}(x, y) = (r^{-1}x, t^{-1}y - st^{-1}r^{-1}x)$ therefore B is invertible. We then check for sideways invertibility with siways map S given by $S(x, y) = (ry, t^{-1}x - t^{-1}sy)$ with inverse $S^{-1}(x, y) = (ty + sr^{-1}x, r^{-1}x)$. Finally, we check for diagonal invertibility, where we have $f(x) = t^{-1}(1 - s)x$ and $g(x) = r(x)$, so $\pi(x) = (g \circ f^{-1})(x) = t(1 - s)^{-1}rx = tr(1 + t^{-1}r^{-1}s)x = (tr + s)x$.

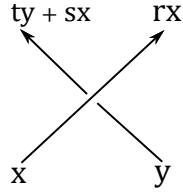
We now have to check that the set-theoretic Yang-Baxter equation is satisfied. We have

$$\begin{aligned} t^2z + tsy + sx &= t^2z + sty + (str + s^2)x \\ r(ty + sx) &= t(ry) + s(rx) \\ r^2x &= r^2x \end{aligned}$$

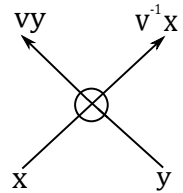
the second equation is satisfied by commutativity in $\tilde{\Lambda}$ and reduces the first equation to $(1 - tr)s = s^2$. \square

Corollary 3 The birack rank of a finite (t, s, r) -birack is the smallest integer $N > 0$ such that $(tr + s)^N = 1$.

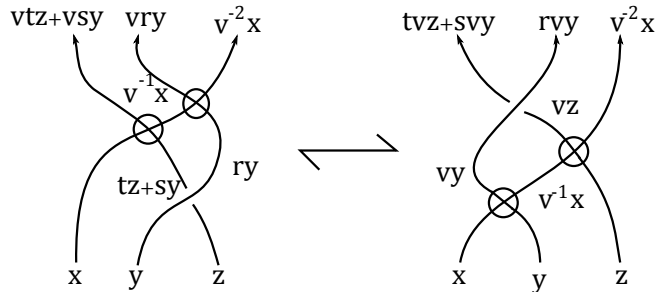
In the classical case we define the operation at the crossing as:



In the case where we do not allow the virtual crossing to be trivial we define the operation at the crossing as:



Where the birack structure needs to satisfy:



where v is invertible.

Remark 1 If we set $r = 1$ we then have a (t, s) -rack which was further studied in [6].

Chapter 3

Twisted Virtual Links

Twisted virtual links were first introduced by Mario O Bourgoïn in [2] and then further studied in works such as [8, 14]. Twisted virtual links extend the concept of *virtual links* from previous work [9, 7]; where virtual links arise by drawing link diagrams on compact orientable surfaces with nonzero genus, twisted virtual links arise when we draw link diagram on compact surfaces allowing nonzero genus and nonzero cross-cap number.

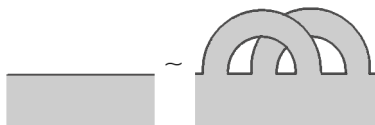
Knot and link diagrams are usually drawn on flat paper without explicitly specifying a supporting surface Σ on which the knot diagram is drawn. If we do explicitly draw Σ , we have a *link-surface* diagram. Often we will remove a disk from $\Sigma \setminus L$ so we can flatten Σ as depicted. Virtual crossings correspond to crossed bands while classical crossings correspond to crossings drawn on Σ .



Geometrically, a twisted virtual link is a stable equivalence class of simple closed curves in an I -bundle, i.e. an ambient space obtained by thickening the surface Σ on which the link diagram is drawn. Here “stable equivalence” means that in addition to ambient isotopy of the link within the thickened surface, we can *stabilize* the surface Σ by adding or deleting handles not containing the link. If we remove a disk from $\Sigma \setminus L$ and flatten the resulting Σ' in the usual way to get



then stabilization moves have the form

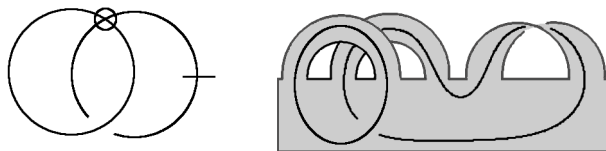


We can represent twisted virtual links combinatorially without having to draw the supporting surface Σ by representing crossings arising from genus in Σ with circled self-intersections known as *virtual crossings* and representing places where our link traverses a cross cap in Σ with a small bar.



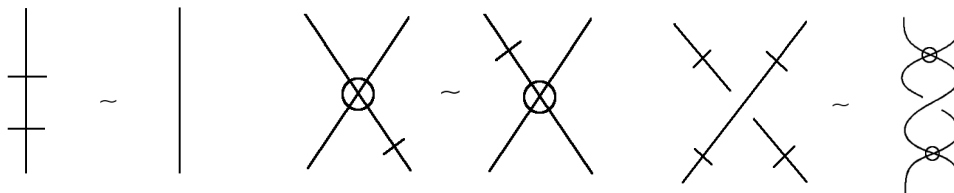
Figure 3.1: Virtual crossing arising from genus and twisted crossing where the link traverses a cross cap, respectively

Then for instance the twisted virtual Hopf link diagram below corresponds to the link-surface diagram shown.

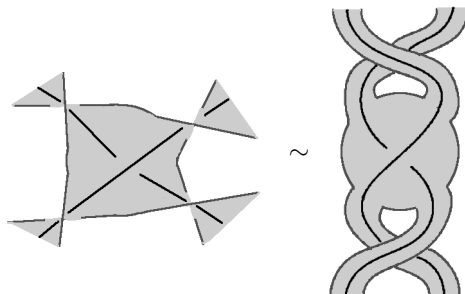


The portions of a twisted virtual link diagram L between over-crossings, undercrossings, virtual crossings and bars are *semiarcs*. For instance, the twisted virtual Hopf link diagram above has six semiarcs.

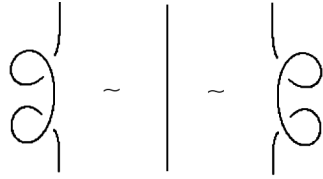
In [2] it is shown that stable isotopy of twisted virtual links corresponds to the equivalence relation on twisted virtual link diagrams generated by the *twisted virtual Reidemeister moves*:



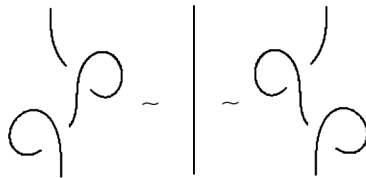
Each of these moves can be understood in terms of link-surface diagrams or abstract link diagrams; for instance, the last move looks like:



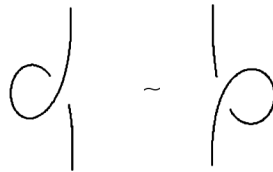
Replacing the usual classical Reidemeister type I move with the blackboard framed type I moves



yields *blackboard framed twisted virtual isotopy*. Including orientations on the link components gives *oriented blackboard framed twisted virtual isotopy*. Note that the move



requires only Reidemeister type II and III moves, and combining this move with the blackboard-framed type I move yields the equivalent move below; see [4].

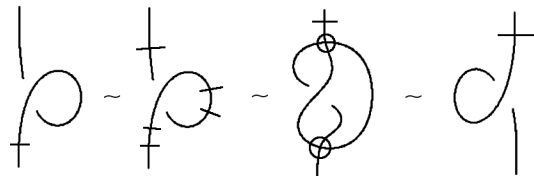


We will primarily be interested in using invariants of oriented blackboard framed twisted virtual isotopy to define an invariant of oriented unframed twisted virtual isotopy analogous to [12] and [13].

We will find the following observations useful in the next section.

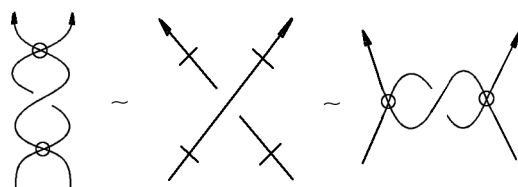
Lemma 4 *A twist bar can be moved past a classical kink.*

Proof.

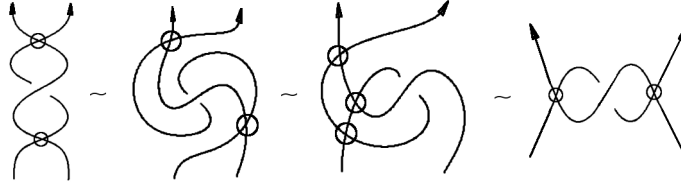


□

Lemma 5 *The two oriented versions of the last twisted virtual move are equivalent, i.e we have*



Proof.



□

3.1 Twisted Jones Polynomial

Just as in the previous case, we use a state sum to defined the *twisted Jones polynomial* of a twisted link as an element of $\mathbb{Z}[A^\pm, M]$, where M counts the number of circles with an odd number of bars in a given diagram.

Theorem 6 If a twisted link diagram is that of a virtual link then it's twisted Jones polynomial is $-A^{-2} - A^2$ times its Jones polynomial, and similarly the twisted Jones polynomial is invariant of twisted links.

The link is not a virtual link if the polynomial of a twisted link has an M variable. If a link has an odd number of bars on its edges then we can factor one M variable from its polynomial. For example, the knot in Figure 3.2 is a onefoil knot in a thickened Klein bottle, and it's twisted Jones polynomial is:

$$V(A, M) = A^{-6} + (1 - M^2)A^{-2}$$

which does not have an M factor and its Jones polynomial is trivial.

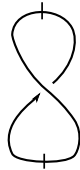


Figure 3.2: A twisted onefoil knot

3.2 Twisted Virtual Biracks

We begin with a definition slightly modified from [14].

Definition 12 Let X be a set and $\Delta : X \rightarrow X \times X$ the diagonal map $\Delta(x) = (x, x)$. A *twisted virtual birack* is a set X with invertible maps $B : X \times X \rightarrow X \times X$, $V : X \times X \rightarrow X \times X$ and an involution $T : X \rightarrow X$ satisfying

- (i) B and V are *sideways invertible*: there exist unquie invertible maps $S : X \times X \rightarrow X \times X$ and $vS : X \times X \rightarrow X \times X$ such that for all $x, y \in X$ we have

$$S(B_1(x, y), x) = (B_2(x, y), y) \quad \text{and} \quad vS(V_1(x, y), x) = (V_2(x, y), y);$$

- (ii) The compositions $S_k^{\pm 1} \circ \Delta$ and $vS_k^{\pm 1} \circ \Delta$ are bijections for $k = 1, 2$;
- (iii) $(vS \circ \Delta)_1 = (vS \circ \Delta)_2$;

(iv) B and V satisfy the set-theoretic Yang-Baxter equations:

$$(B \times \text{Id}_X)(\text{Id}_X \times B)(B \times \text{Id}_X) = (\text{Id}_X \times B)(B \times \text{Id}_X)(\text{Id}_X \times B),$$

$$(V \times \text{Id}_X)(\text{Id}_X \times V)(V \times \text{Id}_X) = (\text{Id}_X \times V)(V \times \text{Id}_X)(\text{Id}_X \times V),$$

and

$$(B \times \text{Id}_X)(\text{Id}_X \times V)(V \times \text{Id}_X) = (\text{Id}_X \times V)(V \times \text{Id}_X)(\text{Id}_X \times B);$$

(v)

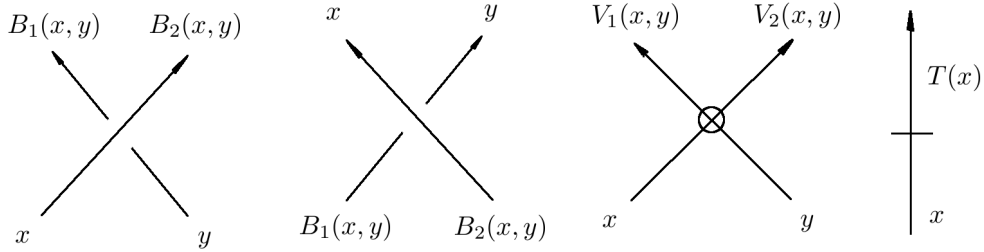
$$(T \times \text{Id})V = V(\text{Id} \times T) \quad \text{and} \quad (\text{Id} \times T)V = V(T \times \text{Id}),$$

(vi)

$$(T \times T)B(T \times T) = VBTV.$$

If we also have $(S \circ \Delta)_1 = (S \circ \Delta)_2$, X is a *twisted virtual biquandle*.

The twisted virtual birack axioms are obtained from the blackboard-framed twisted virtual Reidemeister moves using the following semiarc-labeling scheme:



See [14] for more details.

Just as with other algebraic structures we have the following notions:

Let X and Y be twisted virtual biracks with maps B_X, V_X, T_X and B_Y, V_Y, T_Y respectively, then:

- A map $f : X \rightarrow Y$ is a *homomorphism of twisted virtual biracks* if $B_Y \circ (f \times f) = (f \times f) \circ B_X$, $V_Y \circ (f \times f) = (f \times f) \circ V_X$ and $T_Y \circ f = f \circ T_X$, and
- If $Y \subset X$, then Y is a *twisted virtual subbirack* of X provided $B_Y = B_X \circ I$, $T_Y = T_X \circ I$, and $T_Y = T_X \circ I$ where $I : Y \rightarrow X$ is inclusion.

Remark 2 If X is a twisted virtual birack, then the map B defines a birack structure on X and the map V defined a semiquandle structure on X . Then a birack structure with a compatible semiquandle structure, a *virtual birack*, is defined by the pair B, V . Therefore a twisted virtual birack is a virtual birack with a compatible twist map T . See [15, 11]

Example 6 Let X be a commutative ring with $t, r \in X^*$ and $s \in X$ satisfying $s^2 = (1 - tr)s$; then X is a birack with $B(x, y) = (ty + sx, rx)$ known as a (t, s, r) -birack, see [13]. If we choose $v, w \in X^*$, $u \in X$ satisfying $u^2 = (1 - vw)u$ and set $V(x, y) = (vy + ux, wx)$, then $V^2 = \text{Id}$ requires that

$$x = (vw + u^2)x + uv y \quad \text{and} \quad y = vwy + wux$$

which implies $w = v^{-1}$ and $u = 0$. Notice that $u^2 = 0^2 = (1 - 1)0 = (1 - uv)u$. Therefore our virtual operation becomes $V(x, y) = (vy, v^{-1}x)$. Then for the mixed virtual move multiplication by v requires that it commutes with multiplication by t, s and r .

Selecting $T \in X$ so that $T : X \rightarrow X$ by $T(x) = Tx$, then $T^2 = 1$ is required by the twisted moves. Multiplication by v commutes with multiplication by T , and

$$T^2rx = rx = v^{-2}tx + sy, \quad v^2ry = T^2ty + T^2sx = ty + sx$$

need to be satisfied.

By looking at coefficients, we see that we need $s = 0$ and $v^2r = t$. Since $s = 0$ implies that $s^2 = (1 - tr)s$, the conditions on our coefficients reduce to $t, r, v, T \in X^*$ with $T^2 = 1$ and $v^2r = t$. Therefore for any commutative ring X with units t, r, v, T satisfying the preceding conditions, we have a twisted virtual birack structure on X defined by

$$B(x, y) = (ty, rx), \quad V(x, y) = (vy, v^{-1}x), \quad \text{and} \quad T(x) = Tx.$$

Example 7 We can represent a twisted virtual birack structure on a finite set $X = \{x_1, \dots, x_n\}$ with an $n \times (4n + 1)$ -matrix $M_X = U|L|vU|vL|T$ with $n \times n$ blocks U, L, vU, vL encoding the operations B, V and an $n \times 1$ block T encoding the involution T in the following way:

- if $B(x_i, x_j) = (x_k, x_l)$ we set $U_{ji} = k$ and $L_{i,j} = l$ (note the reversed order of the subscripts in U ; this is for compatibility with previous work);
- if $V(x_i, x_j) = (x_k, x_l)$ we set $vU_{ji} = k$ and $vL_{i,j} = l$, and
- if $T(x_i) = x_j$ we set $T[i, 1] = j$.

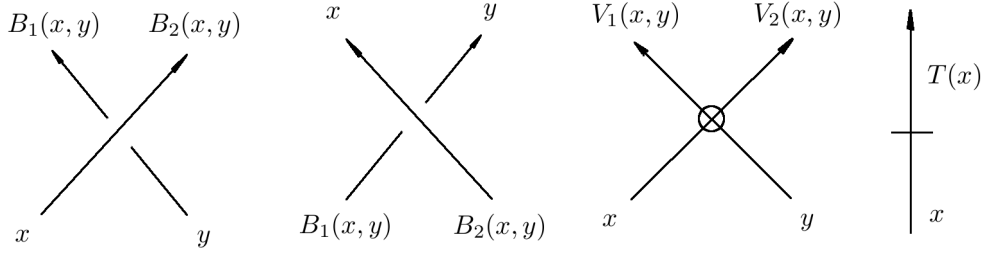
Every finite twisted virtual birack can be encoded by such a matrix, and conversely an $n \times (4n + 1)$ matrix with entries in $\{1, 2, \dots, n\}$ defines a twisted virtual birack provided the twisted virtual birack axioms are all satisfied by the maps B, V and T defined by the matrix.

For instance, our *python* computations reveal that there are eight twisted virtual birack structures on the set $X = \{x_1, x_2\}$, given by the birack matrices

$$\begin{aligned} & \left[\begin{array}{cc|cc|cc|cc} 2 & 2 & 2 & 2 & 1 & 1 & 1 & 1 & 2 \\ 1 & 1 & 1 & 1 & 2 & 2 & 2 & 2 & 1 \end{array} \right], \quad \left[\begin{array}{cc|cc|cc|cc} 2 & 2 & 2 & 2 & 2 & 2 & 2 & 2 & 2 \\ 1 & 1 & 1 & 1 & 1 & 1 & 1 & 1 & 1 \end{array} \right] \\ & \left[\begin{array}{cc|cc|cc|cc} 1 & 1 & 1 & 1 & 1 & 1 & 1 & 1 & 2 \\ 2 & 2 & 2 & 2 & 2 & 2 & 2 & 2 & 1 \end{array} \right], \quad \left[\begin{array}{cc|cc|cc|cc} 1 & 1 & 1 & 1 & 2 & 2 & 2 & 2 & 2 \\ 2 & 2 & 2 & 2 & 1 & 1 & 1 & 1 & 1 \end{array} \right] \\ & \left[\begin{array}{cc|cc|cc|cc} 2 & 2 & 2 & 2 & 1 & 1 & 1 & 1 & 1 \\ 1 & 1 & 1 & 1 & 2 & 2 & 2 & 2 & 2 \end{array} \right], \quad \left[\begin{array}{cc|cc|cc|cc} 2 & 2 & 2 & 2 & 2 & 2 & 2 & 2 & 1 \\ 1 & 1 & 1 & 1 & 1 & 1 & 1 & 1 & 2 \end{array} \right] \\ & \left[\begin{array}{cc|cc|cc|cc} 1 & 1 & 1 & 1 & 1 & 1 & 1 & 1 & 1 \\ 2 & 2 & 2 & 2 & 2 & 2 & 2 & 2 & 2 \end{array} \right], \quad \left[\begin{array}{cc|cc|cc|cc} 1 & 1 & 1 & 1 & 2 & 2 & 2 & 2 & 1 \\ 2 & 2 & 2 & 2 & 1 & 1 & 1 & 1 & 2 \end{array} \right] \end{aligned}$$

3.3 Counting Invariants

Definition 13 Let L be a twisted virtual link diagram and X a twisted virtual birack. A *twisted virtual birack labeling* of L by X , or just an X -*labeling* of L , is an assignment of an element of X to every semiarc in L such that at every classical crossing, virtual crossing, and twist bar we have



The twisted virtual birack axioms are translations of the oriented blackboard-framed twisted virtual Reidemeister moves using the labeling conventions in definition 13. Thus, by construction we have

Theorem 7 *If L and L' are twisted virtually blackboard-framed isotopic twisted virtual links and X is a finite twisted virtual birack, then the number of X -labelings of L equals the number of X -labelings of L' .*

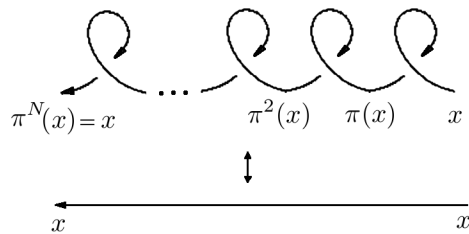
As with quandle labelings of oriented classical links, rack labelings of blackboard-framed classical links, etc., an X -labeling of a twisted virtual link diagram L can be understood as a homomorphism $f : TVB(L) \rightarrow X$ of twisted virtual biracks where $TVB(L)$ is the *fundamental twisted virtual birack* of L . More precisely, let G be a set of symbols, one for each semiarc in L , and define the set of *twisted virtual birack words* in G , $W(G)$, recursively by the rules

- $g \in G \Rightarrow g \in W(G)$,
- $g, h \in W(G) \Rightarrow B_k^{\pm 1}(g, h), S_k^{\pm 1}(g, h), V_k^{\pm 1}(g, h), vS_k^{\pm 1}(g, h), T(g) \in W(G)$ for $k = 1, 2$.

Then the *free twisted virtual birack* on G is the set of equivalence classes in $W(G)$ modulo the equivalence relation generated by the twisted virtual birack axioms, and the *fundamental twisted virtual birack* of L is the set of equivalence classes of elements of the free twisted virtual birack on G modulo the equivalence relation generated by the crossing relations. Both sets are twisted virtual biracks under the operations

$$B([x], [y]) = ([B_1(x, y)], [B_2(x, y)]), \quad V([x], [y]) = ([V_1(x, y)], [V_2(x, y)]), \quad T([x]) = [T(x)].$$

In [13] it is observed that the number of birack labelings of a link diagram is unchanged by the N -*phone cord move* where N is the birack rank of the labeling birack X :



In particular, the number of labelings is periodic in the writhe of each component of L with period N , and consequentially the sum of the numbers of labelings over a complete period of writhes mod N forms an invariant of unframed isotopy. We would like to extend this result to the case of twisted virtual biracks.

Definition 14 Let L be a twisted virtual link with c components and X a twisted virtual birack with rank N . The *integral twisted virtual birack counting invariant* is number of X -labelings of L over a complete period of blackboard framings of $L \bmod N$. That is,

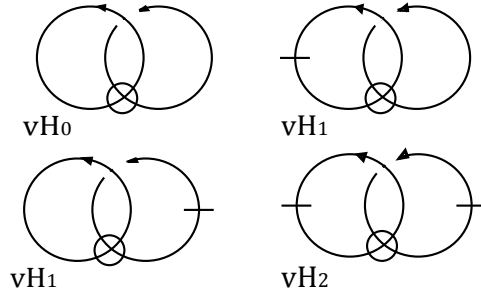
$$\Phi_X^{\mathbb{Z}}(L) = \sum_{\mathbf{w} \in (\mathbb{Z}_N)^c} |\text{Hom}(TVB(L, \mathbf{w}), X)|.$$

By construction, we have

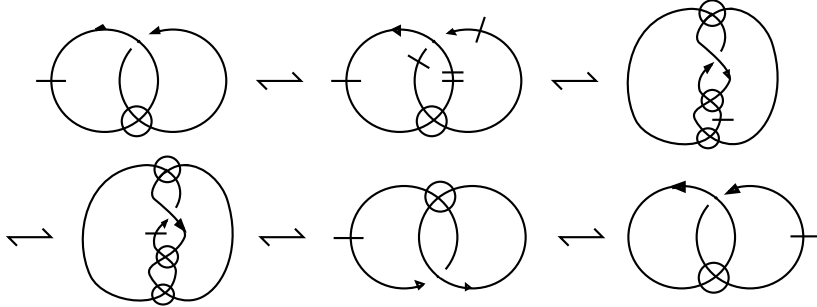
Theorem 8 If L and L' are twisted virtually isotopic twisted virtual links, and X is a finite twisted virtual birack, then $\Phi_X^{\mathbb{Z}}(L) = \Phi_X^{\mathbb{Z}}(L')$.

Starting with a virtual link, one may wonder which placements of twist bars will yield distinct twisted virtual links. As a result of moves tI and tII, we can place at most one twist bar on any portion of the knot between classical semiarcs. The following example illustrates this.

Example 8 The *virtual Hopf link* is the smallest nontrivial virtual knot with two components. Since it has only two semiarcs, there are $2^2 = 4$ potentially different twisted links which project to the virtual Hopf link under removal of twist bars.



Using twisted virtual isotopy moves, we can see that the two forms of vH_1 are equivalent:



An interesting result to notice is that the twist jumps from one component to the other; however, this is less likely to happen in less symmetric links.

We can also use the integral counting invariant $\Phi_X^{\mathbb{Z}}(L)$ with respect to various twisted virtual biracks to show that the links vH_2 , vH_1 and vH_0 are not equivalent. Let X_1 be the twisted virtual birack with matrix

$$M_{X_1} = \left[\begin{array}{cc|cc|cc|cc|cc} 2 & 2 & 2 & 2 & 2 & 2 & 2 & 2 & 2 & 2 \\ 1 & 1 & 1 & 1 & 1 & 1 & 1 & 1 & 1 & 1 \end{array} \right]$$

Then we have $\Phi_{X_1}^{\mathbb{Z}}(vH_0) = 4$, $\Phi_{X_1}^{\mathbb{Z}}(vH_1) = 0$, and $\Phi_{X_1}^{\mathbb{Z}}(vH_2) = 0$. Similarly, let X_2 be the twisted virtual birack with matrix

$$M_{X_2} = \left[\begin{array}{ccc|ccc|ccc|ccc|c} 2 & 2 & 1 & 2 & 2 & 1 & 1 & 1 & 1 & 1 & 1 & 1 & 2 \\ 1 & 1 & 2 & 1 & 1 & 2 & 2 & 2 & 2 & 2 & 2 & 2 & 1 \\ 3 & 3 & 3 & 3 & 3 & 3 & 3 & 3 & 3 & 3 & 3 & 3 & 3 \end{array} \right]$$

Then we have $\Phi_{X_2}^{\mathbb{Z}}(vH_0) = 5$, $\Phi_{X_2}^{\mathbb{Z}}(vH_1) = 3$, and $\Phi_{X_2}^{\mathbb{Z}}(vH_2) = 5$.

3.4 Enhanced Counting Invariants

We close this chapter by looking at the several enhancements of the twisted virtual birack counting invariant just as in the case of biracks. An *enhancement* is generally a stronger invariant that associates an invariant signature to each labeling of a twisted virtual link diagram. Because of this association, instead of simply counting labelings, we collect the signatures to get a multiset whose cardinality recovers the counting invariant. The standard enhancements include the following:

- *Image enhancement.* Given a valid labeling $f : TVB(L) \rightarrow X$ of the semiarcs in a twisted virtual link diagram L of c components by a twisted virtual birack X of rank N , the image of f is an invariant of twisted virtual isotopy. From a labeled link diagram, we can compute $\text{Im}(f)$ by taking the closure under the operations $B_1(x, y)$, $B_2(x, y)$, $V_1(x, y)$, $V_2(x, y)$ and $T(x)$ of the set of all elements of Y appearing as semiarc labels. Then we have an enhanced invariant

$$\Phi_X^{\text{Im}}(L) = \sum_{\mathbf{w} \in (\mathbb{Z}_N)^c} \left(\sum_{f \in \text{Hom}(TVB(L, \mathbf{w}), X)} u^{|\text{Im}(f)|} \right).$$

- *Writhe enhancement.* For this one, we simply keep track of which writhe vectors contribute which labelings. For a writhe vector $\mathbf{w} = (w_1, \dots, w_c)$, let us denote $q^{\mathbf{w}} = q_1^{w_1} \dots q_c^{w_c}$. Then the *writhe enhanced invariant* is

$$\sum_{\mathbf{w} \in (\mathbb{Z}_n)^c} |\text{Hom}(TVB(L, \mathbf{w}), X)| q^{\mathbf{w}}.$$

- *Twisted virtual birack polynomials.* Let X be a finite twisted virtual birack with birack matrix $[M_1|M_2|M_3|M_4|M_5]$. For each element $x_k \in X = \{x_1, \dots, x_n\}$, let $c_i(x_k) = |\{j \mid M_i[x_j, x_k] = x_j\}|$ and let $r_i(x_k) = |\{j \mid M_i[x_k, x_j] = x_k\}|$. Then for any sub-twisted virtual birack $Y \subset X$, the sub-TVG polynomial of Y is

$$p_{Y \subset X} = \sum_{x \in Y} \left(\sum_{i=1}^5 t_i^{c_i(x)} s_i^{r_i(x)} \right).$$

Then for each X -labeling f of L , the sub-twisted virtual birack polynomial of the image of f gives an invariant signature, so we have the *twisted virtual birack polynomial enhanced invariant*

$$\Phi_X^p(L) = \sum_{\mathbf{w} \in (\mathbb{Z}_N)^c} \left(\sum_{f \in \text{Hom}(TVB(L, \mathbf{w}), X)} u^{p_{\text{Im}(f) \subset X}} \right).$$

Bibliography

- [1] L. Kauffman. New Invariants in the Theory of Knots. *American Mathematical Monthly* **95** (1988) 195-242.
- [2] M.O. Bourgoïn. Twisted link theory. *Algebr. Geom. Topol.* **8** (2008) 12491279.
- [3] R. Fenn, M. Jordan-Santana and L. Kauffman. Biquandles and virtual links. *Topology Appl.* **145** (2004) 157-175.
- [4] R. Fenn and C. Rourke. Racks and links in codimension two. *J. Knot Theory Ramifications* **1** (1992) 343-406.
- [5] J.S. Carter, S. Kamada and M. Saito. Geometric interpretations of quandle homology. *J. Knot Theory Ramifications* **10** (2001) 345-386.
- [6] J. Ceniceros and S. Nelson. (t, s) -racks and their link invariants. arXiv:1011.5455
- [7] N. Kamada and S. Kamada. Abstract link diagrams and virtual knots. *J. Knot Theory Ramifications* **9** (2000) 93-106.
- [8] N. Kamada. The polynomial invariants of twisted links. *Topology Appl.* **157** (2010) 220227.
- [9] L. Kauffman. Virtual Knot Theory. *European J. Combin.* **20** (1999) 663-690.
- [10] L. H. Kauffman and D. Radford. Bi-oriented quantum algebras, and a generalized Alexander polynomial for virtual links. *Contemp. Math.* **318** (2003) 113-140.
- [11] L. H. Kauffman and V. O. Manturov. Virtual biquandles. *Fundam. Math.* **188** (2005) 103-146.
- [12] S. Nelson. Link invariants from finite racks. arXiv:1002.3842.
- [13] S. Nelson. Link invariants from finite biracks. arXiv:1002.3842.
- [14] N. Kamada and S. Kamada. Biquandles with structures related to virtual links and twisted links. Preprint.
- [15] A. Henrich and S. Nelson. Semiquandles and flat virtual links. *Pacific J. Math* **248** (2010) 155170.

DEPARTMENT OF MATHEMATICAL SCIENCES,
CLAREMONT MCKENNA COLLEGE,
850 COLUMBIA AVE.,
CLAREMONT, CA 91711